THERMAL PLASMA EXPANSION PROCESS FOR THE CONTROLLED SYNTHESIS OF SILICON, CARBON AND SILICON CARBIDE NANOPARTICLES

D. Hansen, B. Micheel, N. Rao, S. Girshick, J. Heberlein, and P. McMurry

Department of Mechanical Engineering, University of Minnesota
Minneapolis, MN 55455 USA

ABSTRACT

The controlled synthesis of ultrafine silicon, carbon, and silicon carbide particles using a thermal plasma expansion process is experimentally investigated. A dc generated Ar-H_2 thermal plasma is seeded with vapor phase precursors and then quenched in a converging nozzle at rates measuring ~ $5x10^6$ K/s. Enthalpy probe measurements, calorimetric energy balances, and extensive nozzle wall temperature data facilitate the characterization of the plasma gas temperature and velocity. On-line size classification of aerosol samples extracted downstream of the nozzle exit indicate that 90% of the Si and SiC particles are ≤ 16 nm in diameter.

INTRODUCTION

Nanophase materials having domain sizes less than 100 nm hold the potential for improved material properties that differ greatly from their bulk counterparts, including improved hardness, ceramic ductility, and intriguing electrical, magnetic, and optical properties. One effective method for the generation of these ultrafine particles is gas phase synthesis in a thermal plasma. Thermal plasmas offer fast reacting environments for the dissociation of reactants while simultaneously providing the high quench rates conducive to the nucleation and growth of nanosized particles [1]. Previous research in this area has typically utilized cold gas mixing to achieve these supercooled conditions. This method however has the disadvantage of strong two-dimensional non-uniformities in the quench region which result in complex vapor volume trajectories and subsequent variations in particle size. To overcome this problem, a dc thermal plasma expansion reactor was constructed which utilizes a converging nozzle to supersaturate vapor precursors in a well controlled and characterized process. This unique approach provides essentially uniform radial temperature and velocity profiles while retaining high quench rates in the axial direction. Previously reported particle distributions of samples collected downstream in the jet centerline indicate that 90% of the detected Si and SiC particles are smaller than 16 nm and are well approximated by log-normal distributions with a relatively low geometric standard deviation of 1.6 [2]. This paper

expands upon these promising findings through further characterization of the plasma conditions and by investigating particle coagulation and growth in the jet downstream of the nozzle.

PLASMA CHARACTERIZATION MEASUREMENTS

Schematics of the thermal plasma reactor system and in situ particle characterization instruments are displayed in Fig. 1. The core of the continuous flow reactor consists of three functional and calorimetrically independent zones: a dc plasma torch configured for Ar-H_2 operation, a 2.5 cm long reactant injection ring, and a 5 cm long converging nozzle. The injection ring and nozzle are lined with a removable insert consisting of a continuous piece of specially machined boron nitride rod. The internal flow geometry of the boron nitride liner is defined by a 15 mm injection ring inlet diameter, a converging nozzle section optimized for a uniform cooling rate, and a nozzle exit diameter of 5 mm. Dissociation of the $SiCl_4$ and/or CH_4 reactants inside the injection ring yield the necessary gas phase precursors. This reacting mixture is then rapidly accelerated in the nozzle, resulting in supersaturation and nucleation of Si and/or SiC nanoparticles. This particle-laden jet exhausts into a cooled, subatmospheric diagnostics chamber where it is sampled by a two-stage ejector dilution probe and then routed to the particle diagnostic instrumentation.

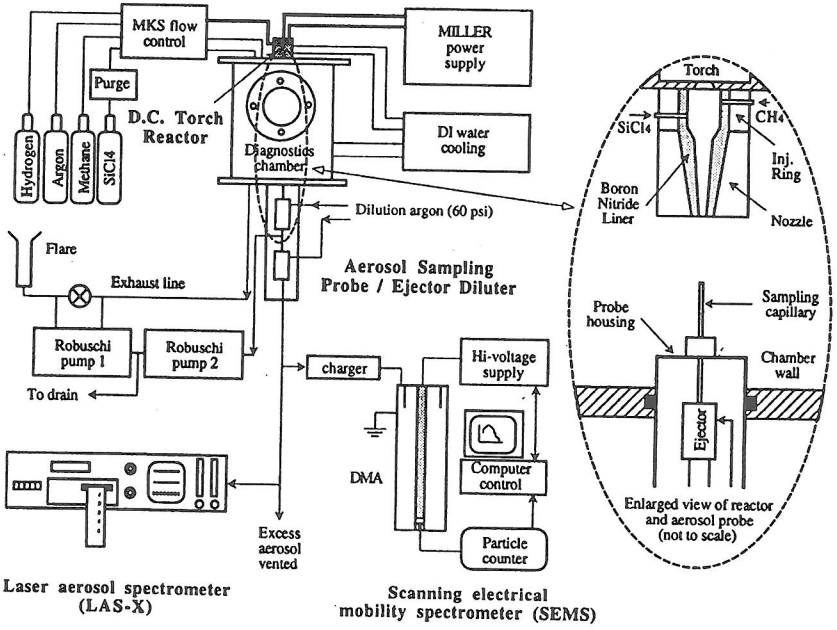

Figure 1. Schematic of dc plasma expansion reactor for nanoparticle synthesis

Typical operating conditions and gas flow rates are given in Table 1. For silicon nanoparticle synthesis, only $SiCl_4$ is injected, whereas silicon carbide production

requires the additional reactant CH_4. For carbon particle generation, only CH_4 is injected and H_2 is eliminated from the feed gas as it suppresses the formation of carbon particles.

Table 1 - Experimental operating conditions

Arc current	150-250 A
Arc voltage	18-65 V
Nozzle inlet pressure / exit pressure	67-101 kPa / 53.3 kPa
Argon flow rate / Hydrogen flow rate	30-40 slm / 0-10 slm
Silicon tetrachloride flow rate	0.05-0.07 slm
Methane flow rate	0.1-1 slm

Our experimental plasma characterization focuses on gas temperature and velocity measurements within the reactor and on liner wall temperature data. Calorimetric measurements yield average enthalpy and velocity profiles at the torch, injection ring, and nozzle exits while an enthalpy probe provides local measurements. Radial enthalpy probe data at the nozzle exit confirm a uniform, essentially one-dimensional flow field and also independently verify the values obtained calorimetrically [2,3]. Consequently, energy balances provide robust, reliable representations of the flow field in the particle production region. Representative values of the plasma temperature, enthalpy, and velocity at selected axial locations are tabulated in Table 2 for several different operating conditions.

Table 2 - Average temperature and velocity data (± experimental uncertainties)

Operating Conditions			**Temperature [K]**			**Velocity [m/s]**		
Current/Ar Flow/H_2 Flow [A] / [slm] / [slm]			Torch exit	Inj. Ring exit	Nozzle exit	Torch exit	Inj. Ring exit	Nozzle exit
150	40	0	3300±80	3820±90	1850±50	161±3	125±4	430±10
250	40	0	5000±200	4200±200	2570±70	222±8	171±9	600±20
200	30	0	4000±300	3800±300	2400±200	180±10	140±10	420±30
			Enthalpy measurements [J/kg]					
200	30	7.5	$6.1\pm.5\times10^6$	$4.5\pm.3\times10^6$	$2.1\pm.2\times10^6$			
Temperature and velocity measurements assuming chemical equilibrium								
			4600±500	3700±100	2700±200	260±30	180±10	600±50

The data for the Ar-H_2 plasma are listed according to enthalpy values, with reference temperature and velocity profiles also given assuming chemical equilibrium. Partially frozen flow conditions in the nozzle are expected as a result of the rapid

quench rates (~ $5x10^6$ K/s). To this end, a numerical model is being developed which simulates nozzle flow conditions and accounts for homogeneous and heterogeneous hydrogen recombination. Preliminary results indicate partially frozen flow conditions are present, with the net effect being a 5-10% reduction in the nozzle exit temperature and velocity values when compared to chemical equilibrium calculations [3].

Additional insight into the plasma conditions can be obtained from liner wall temperature measurements. A specially designed liner was constructed in which miniature thermocouples were embedded at various axial and radial locations in the injection ring and nozzle walls. Characterization and control of the inner wall temperature is crucial to ensuring the minimization of radial temperature gradients (and subsequent nonuniformities in the gas flow) and for preventing wall condensation. Thermal control is exerted by systematically modifying the contact resistance between the boron nitride insert and its cooling circuits. Fig. 2 depicts temperatures measured within the liner at axial locations near the injection ring inlet and nozzle exit, with corresponding inner wall surface temperatures estimated to be several hundred degrees hotter than the values shown [3]. The 'cold nozzle' data is representative of an unmodified liner whereas the 'hot nozzle' data clearly shows the temperature enhancement and axial uniformity achieved through these modifications.

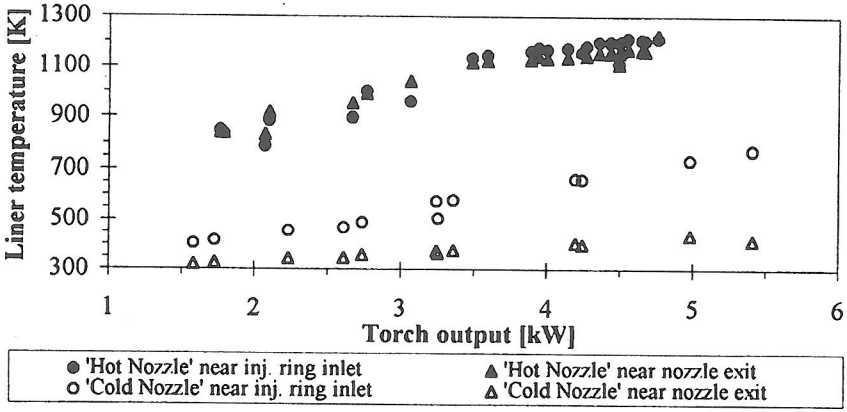

Figure 2. Boron nitride liner temperatures versus torch output (where torch output is defined as the total stagnation enthalpy of the exiting plasma)

Preliminary particle production runs with the 'hot nozzle' showed significant decreases in wall condensation and in associated nozzle clogging.

PARTICLE CHARACTERIZATION MEASUREMENTS

Particle characterization is accomplished by sampling aerosols from various axial and radial locations immediately downstream of the nozzle exit using a two-stage ejector dilution probe connected to a scanning electrical mobility spectrometer (SEMS) and laser aerosol spectrometer (LAS-X) (see Fig. 1). The SEMS instrumentation

permits on-line measurement of the particle size distribution for particles 4-120 nm in diameter with the LAS-X providing a similar capability for larger particles (0.12-3 μm in diameter) [4]. Recent studies utilizing these aerosol diagnostics techniques have focused on the axial and radial dependence of particle coagulation and growth in the jet. On-axis SEMS measurements 40 mm downstream of the nozzle exit show particle size distributions with number-mean diameters of 7.5 nm, whereas samples extracted 125 mm away exhibit 11-14 nm number-mean diameters as a result of longer growth times in the jet [4]. Radial scans of the aerosol jet during silicon production were also taken 125 mm downstream of the nozzle exit and are shown in Fig. 3 for the base operating case of 30 slm of Ar, 7.5 slm of H_2, and ≈ 0.06 slm of $SiCl_4$ at 200 A of arc current.

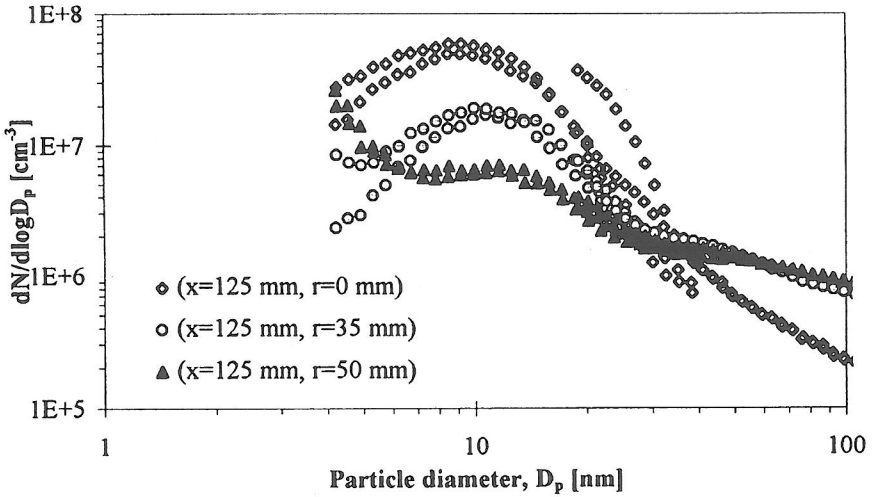

Figure 3. Number density distribution functions ($dN/d\log D_p$) for Si particles at various radial locations 125 mm downstream of the nozzle exit

At increasing radial distances, the distribution shifts from smaller particles nucleated and grown in the nozzle to larger agglomerates formed in the recirculating chamber gas and subsequently entrained in the jet fringes by turbulent mixing. These two different sources yield a bimodal particle size distribution which is readily visible in Fig. 4, where on-axis SEMS and LAS-X data have been combined for Si production under the base operating conditions. The interlinking curve represents an estimate of the actual number distribution, with the downward trend for the LAS-X data in the 0.1-0.3 μm range being attributed to a decreased detection efficiency at smaller sizes. These number distributions indicate that 90% of the particles are below 16 nm. In contrast, particle mass distributions (not shown here) indicate that nanoparticles less than 100 nm in diameter contain only ~ 25% of the total mass [4]. An accompanying paper [5] presents supportive numerical modeling work of the particle nucleation in the nozzle and subsequent coagulation and growth in the free jet expansion.

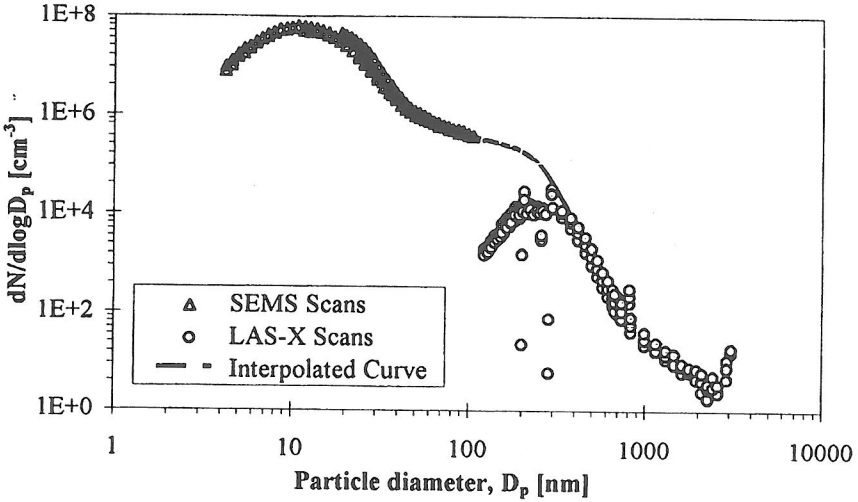

Figure 4. Combined SEMS and LAS-X number density distribution functions ($dN/d\log D_p$) for on-axis Si particles sampled 125 mm downstream of the nozzle exit

CONCLUSION

A well characterized plasma expansion process for the uniform gas phase synthesis of silicon, carbon, and silicon carbide nanoparticles has been described. Particles generated by this process have narrow size distributions which tend to increase in mean diameter and inhomogeneity (due to coagulation and agglomeration effects) for movements away from the nozzle exit. Future research is targeted at minimizing this coagulation and large agglomerate formation.

ACKNOWLEDGMENTS

The authors gratefully acknowledge support for this research from the National Science Foundation (NSF/ECS-9118100) and the Minnesota Supercomputer Institute.

REFERENCES

1. S. L. Girshick and C.-P. Chiu, *Plasma Chem. Plasma Process.* **9**, 355-369 (1989).

2. N. Rao, S. Girshick, J. Heberlein, P. McMurry, M. Bench, S. Jones, D. Hansen, and B. Micheel, accepted for publication, *Plasma Chem. Plasma Proc.* (1995).

3. D. J. Hansen, M.S. thesis, University of Minnesota, 1995.

4. B. A. Micheel, M.S. thesis, University of Minnesota, 1995.

5. B. Micheel, D. Hansen, N. Rao, S. Girshick, J. Heberlein, and P. McMurry, *12th ISPC Proceedings*, Aug. 21-5, 1995.